HHS Public Access

Author manuscript

IEEE Magn Lett. Author manuscript; available in PMC 2021 March 18.

Published in final edited form as:

IEEE Magn Lett. 2016 ; 7: . doi:10.1109/lmag.2015.2508006.

Controlling Iron Oxide Nanoparticle Clustering Using Dual Solvent Exchange Coating Method

Travis A. Meyer[1], **Christopher A. Quinto**[1], **Gang Bao**[1,2]

[1]Wallace H Coulter Department of Biomedical Engineering, Georgia Institute of Technology and Emory University, Atlanta, GA 30322, USA

[2]Department of Bioengineering, Rice University, Houston, TX 77030, USA

Abstract

Superparamagnetic iron oxide nanoparticles (SPIOs) have considerable promise for magnetic resonance imaging, drug/gene delivery, and hyperthermia applications. It has been shown recently that self-assembly of SPIOs into large superstructures can have a significant impact on their magnetic properties and functionality. In this work, we developed a novel method for controlling the clustering of SPIOs with two different core sizes (8 nm and 15 nm) by varying the amount of amphiphilic coating molecules used during the dual solvent exchange coating process. We show that hydrodynamic size and T_2 relaxivity can be increased using this approach, while the specific absorption rate is decreased. These results demonstrate a new, simple method for triggering the self-assembly of SPIO clusters using commercially available and biocompatible phospholipid-poly(ethylene glycol) conjugates.

Index Terms—

Nanomagnetics; Clustering; Hyperthermia; Iron Oxide Nanoparticles; Relaxivity

I. INTRODUCTION

Superparamagnetic iron oxide nanoparticles (SPIOs) have received significant attention in the past two decades as potential drug/gene delivery vehicles, MRI contrast agents, and magnetic hyperthermia mediators due to their unique magnetic properties, high biocompatibility, and ease of synthesis [Gupta 2005]. Considerable efforts have been made to produce high-quality SPIOs with improved magnetic properties – notably high T_2 relaxivity for MRI contrast and high specific absorption rate (SAR) for magnetic fluid hyperthermia, both are important in developing SPIOs for a broad range of biomedical applications [Lee 2015].

In addition to improving the quality of synthesis for individual SPIOs, recent work has demonstrated that controlling the self-assembly of nanoparticles can have a significant impact on magnetic properties, including T_2 relaxivity and SAR [Shtykova 2007, Meteria

Corresponding author: G. Bao (gang.bao@rice.edu).

2014, Sadat 2014]. By controlling the size and shape of the final nanoparticle assemblies, T_2 relaxivity and SAR can be altered to match the intended application. However, the majority of the techniques used to facilitate self-assembly utilize non-biocompatible materials, are technically challenging, and/or require complicated synthesis of di-block or tri-block copolymers.

In this work, we demonstrate a new, simple method to control clustering of SPIOs using commercially available, biocompatible materials through the dual solvent exchange coating method [Tong 2011]. This technique involves the gradual increase of the environment polarity through a two-step solvent exchange process, which drives the micellization of an amphiphilic molecule, typically a phospholipid-poly(ethylene glycol) (PEG) conjugate, onto the surface of the hydrocarbon-stabilized iron oxide cores through hydrophobic interactions. By controlling the ratio of amphiphilic molecules to iron oxide cores during the coating process, we show that clustering of the nanoparticles can be induced, leading to colloidally-stable nanoparticles with a range of hydrodynamic diameters. We then characterized the T_2 relaxivity and SAR of the clustered SPIOs, demonstrating the ability to modulate these parameters post-nanoparticle synthesis. This work demonstrates a novel, simple method for controlling the self-assembly of individual SPIOs into larger clusters that show promise as high-sensitivity MRI contrast agents.

II. EXPERIMENTAL METHODS

A. Iron Oxide Nanoparticle Core Synthesis and Coating

Iron oxide cores were synthesized using the thermal decomposition method established by Sun et al [2003], using iron(III) acetylacetonate as the precursor, benzyl ether as the solvent, and oleic acid and oleylamine as the surfactants. The initial 8 nm iron oxide cores were then used to produce 15 nm cores through seed-mediated growth [Sun 2003].

To render the as-synthesized iron oxide cores water soluble, the dual solvent exchange coating method was utilized. Briefly, 200 μL of iron oxide cores (5 mg Fe/mL in toluene) was added to 800 uL of chloroform with differing amounts of 1,2-distearoyl-sn-glycero-3-phosphoethanolamine-N-[methoxy(polyethylene glycol)-2000] (DSPE-PEG), ranging from 0.5 mg (0.5:1 w/w DSPE-PEG:Fe coating ratio) to 4 mg (4:1 coating ratio). 4 mL of DMSO was added dropwise to the solution over 30 minutes in an argon environment. Chloroform and toluene were then removed under vacuum, followed by addition of 16 mL of de-ionized water over 30 minutes using a syringe pump. The mixture was substituted with fresh water using three rounds of centrifugation in centrifugal filter tubes (Vivaspin 20, 100kDa MWCO). Finally, empty micelles were removed by three rounds of ultracentrifugation (100,000 x*g*, 1 hour).

B. Characterization

Iron concentrations were measured using the colorimetric ferrozine assay [Stookey 1970].

Transmission electron microscopy (TEM) was used to determine the size and shape of the iron oxide cores after synthesis. Briefly, 5 μL of as-synthesized cores in toluene (~ 40 μg

Fe/mL) were drop-cast onto carbon coated TEM grids. Images were recorded using a HT7500 microscope (Hitachi) operating at 75 kV attached to a CCD camera.

Magnetization measurements were carried out at 300K on powered samples with an external magnetic field in the range of 0-5 x 10^4 gauss using a SQUID magnetometer (Quantum Design). Saturation magnetization was calculated using iron content, as measured using the ferrozine assay.

Dynamic light scattering (DLS) was used to investigate the hydrodynamic diameters of the coated iron oxide nanoparticles. Samples were diluted to 100 μg Fe/mL in de-ionized water and filtered using a 0.2μm syringe filter to remove dust particles. Measurements were taken at 25°C using a DynaPro Nanostar DLS instrument (Wyatt). The intensity weighted distribution was reported, along with the Z-average diameter and percent polydispersity from a cumulants analysis.

The effect of aggregation on MR contrast was measured using a 0.47 T Minispec Analyzer MQ20 (Bruker). The transverse relaxation times of SPIOs (concentrations from 1 μg Fe/mL to 10 μg Fe/mL) were recorded at 40°C using the Hahn spin-echo method. T_2 relaxivity (R_2) was calculated by plotting $1/T_2$ against the molar concentration of iron and calculating the slope using linear regression

Magnetic fluid hyperthermia heating efficiency was analyzed by measuring the temperature rise when samples were exposed to an alternating magnetic field (355 kHz, 23.77 kA/m) generated by a 7.5-turn, 2.54 cm inner diameter inductor coil. A 1 mL aqueous suspension of SPIOs (400 μg Fe/mL) was placed inside the coil with polystyrene insulation, and the temperature was measured in real time using a fiber optic temperature probe. The slope of the linear region of the temperature vs. time plot was calculated using linear regression and normalized to a water sample. The specific absorption rate (SAR) was calculated using the equation

$$SAR\left(\frac{W}{g}\right) = \frac{C_p \times m_{H2O} \times \Delta T / t}{m_{Fe}}$$

where C_p is the specific heat of water, m_{H2O} is the mass of water, $\Delta T/t$ is the normalized slope of the temperature vs. time plot, and m_{Fe} is the mass of iron.

All presented values represent 3 independent measurements of a single sample. Error bars represent the standard deviation of these measurements.

III. RESULTS AND DISCUSSION

SPIO cores were synthesized using the thermal decomposition method in benzyl ether with $Fe(acac)_3$ as the metal precursor [Sun 2003]. The synthesized particles were monodisperse with diameters of 8.2 ± 1.6 nm and 15.1 ± 2.2 nm as measured by TEM (Fig. 1). The particles displayed superparamagnetic properties, with magnetic saturation values of 88.4 and 89.6 emu/g Fe for 8 nm and 15 nm SPIOs, respectively, as measured using a SQUID magnetometer.

A. Induced Clustering of SPIOs During Coating

We sought to investigate if the self-assembly of SPIOs into clusters could be driven by modifying the dual-solvent exchange coating technique. The dual-solvent exchange process works by altering the surface energy of the iron oxide cores through changes in the polarity of the environment. This increases the strength of hydrophobic interactions between the hydrocarbon ligands on the nanoparticle surface and the phospholipid block of DSPE-PEG, driving self-assembly into the final core-shell structure in a process analogous to the formation of micelles. We had previously observed that larger coating ratios (defined as the mass ratio of DSPE-PEG to iron in the coating reaction) were necessary to stabilize smaller iron oxide cores. This is presumably due to their higher total surface area per mass of iron (i.e. higher surface area to volume ratio) - an increased amount of DSPE-PEG was needed to stabilize the increased hydrophobic surface area. This inspired us to attempt to shift the equilibrium of the system by purposefully using lower coating ratios, such that DSPE-PEG would no longer be in sufficient quantity to stabilize the entire surface area of cores as single entities. We hypothesized this would force the nanoparticles to cluster within the DSPE-PEG shell in an effort to minimize their surface energy and reduce the total surface area to be stabilized by DSPE-PEG.

Two different sizes of iron oxide cores (8 nm and 15 nm) were coated at different DSPE-PEG:Fe coating ratios (from 0.5:1 to 4:1 w/w), and the resulting nanoparticles were analyzed using dynamic light scattering. We found that lower coating ratios resulted in larger hydrodynamic diameters, indicative of core clustering induced by the coating process (Fig. 2). The average hydrodynamic diameter and polydispersity index for the samples are presented in Table 1. We only show results for two coating ratios which produced singly-dispersed cores (4:1 and 2:1 for 8 nm cores, 2:1 and 1:1 for 15 nm cores), and two coating ratios which produced clustered systems (1:1 and 0.75:1 for 8 nm cores, 0.75:1 and 0.5:1 for 15 nm cores). When coating ratios were normalized based on iron oxide core surface area, it can be seen that both iron oxide cores begin to cluster when the coating ratio is less than 2 DSPE-PEG molecules per nm^2 (Fig. 3).

This value compares favorably with Tong et al [2011], who calculated that 6.5 nm iron oxide cores coated at a 1:1 DSPE-PEG:Fe ratio had a surface coverage of ~1.6 DSPE-PEG molecules per nm^2 for singly-dispersed nanoparticles. The formation of empty micelles during coating is likely a competing process, which reduces the nominal amount of DSPE-PEG available for coating the iron oxide cores, such that an initial loading ratio of ~2 DSPE-PEG molecules per nm^2 is unlikely to be the final density of DSPE-PEG on the nanoparticle surface. It appears that if the amount of DSPE-PEG available for coating is insufficient to reach particular surface coverage, the particles cluster together to reduce their exposed surface area. The fewer DSPE-PEG molecules present initially, the greater the extent of clustering when the solution reaches equilibrium.

B. Effect of Clustering on T_2 Relaxivity

Next, we examined how SPIO clusters created with our technique could be used as MRI contrast agents. Iron oxide nanoparticles generate MR contrast by shortening the transverse relaxation of water protons in their vicinity. This can be quantified by the relaxativity R_2

(defined as the decrease in the characteristic relaxation time T_2 per concentration of iron). Figure 3 shows the R_2 values for both 8 nm and 15 nm cores coated at different DSPE-PEG:Fe coating ratios. As expected, 15 nm cores showed higher relaxivity values compared to 8 nm cores, consistent with previous results [Jun 2005]. For 8 nm cores (Fig. 4A), singly-dispersed cores (4:1 and 2:1 coating ratios) showed similar R_2 values (94 and 89 $mM^{-1}s^{-1}$, respectively), while the clusters showed higher R_2 values up to 165 $mM^{-1}s^{-1}$ (0.75:1 coating ratio). The same trend was observed for 15 nm cores (Fig. 4B), with R_2 values ranging from 269 $mM^{-1}s^{-1}$ for singly-dispersed cores (2:1 and 1:1 coating ratio), up to 634 $mM^{-1}s^{-1}$ for the largest clusters (0.5:1 ratio), comparable to that obtained by Lee et al [2012].

Outer sphere theory predicts that R_2 values increase as particle size increases, known as the motional averaging regime (MAR), due to an increase in the local magnetic field homogeneities that lead to dephasing of water protons in the vicinity of the particles [Brooks 2002]. Monte-Carlo simulations of magnetic nanoparticle clusters by Matsumoto et al. [2008] demonstrate increased R_2 with increasing aggregate size, as these clustered particles are believed to behave magnetically as single large spheres. The increase in R_2 due to nanoparticle clustering has been achieved experimentally by other groups, but the techniques utilized to drive self-assembly involve the use of di-block or tri-block copolymers synthesized in-house [Balasubramaniam 2014, Berret 2006, Poselt 2012]. This increases the complexity of the method, decreasing the accessibility for other labs and increasing potential regulatory hurdles. The technique presented here uses commercially available and FDA-approved DSPE-PEG, which simplifies the overall process. Furthermore, the R_2 value of 634 $mM^{-1}s^{-1}$ for the largest cluster of 15 nm SPIO cores is among the highest ever reported.

C. Effect of Clustering on SAR

Finally, we investigated the potential of the clustered SPIOs to act as mediators for magnetic fluid hyperthermia. When placed in an alternating magnetic field, superparamagnetic nanoparticles experience relaxation losses (either Néelian or Brownian) which dissipate heat into the surrounding environment [Laurent 2011]. This heat generation can be quantified by the specific absorption rate (SAR), which describes the power output per mass of particles. The SAR was calculated by measuring the temperature increase of an aqueous solution of particles over time when exposed to AMF (355 kHz, 23.77 kA/m) (Fig. 4). As with T_2 relaxivity, we found that 15 nm cores showed higher SAR values compared to 8 nm cores, consistent with previous work [Gonzalez-Weimuller 2009, Salas 2014].

For 8 nm cores (Fig. 4A), SAR values decreased with increasing cluster size from 147 W/g to 67 W/g for coating ratios of 4:1 and 0.75:1, respectively. 15 nm cores showed a similar trend (Fig. 4B), with SAR values decreasing from 616 W/g to 133 W/g for coating ratios of 2:1 and 0.5:1, respectively.

While there is still debate about the effect SPIO clustering has on SAR, the results here are consistent with the majority of those in the literature using similar systems [Andreu 2015, Etheridge 2014], but differ from results obtained using a “nano-flower” architecture [Hugounenq 2012]. Both experimental and theoretical work have demonstrated that increased dipole-dipole interactions, which is likely to occur in clustered nanoparticle systems, lead to decreased heat output [Haase 2012, Branquinho 2013]. Urtizberea et al

[2010] found that increasing nanoparticle concentration (and thus increasing dipole-dipole interactions) decreased Néelian relaxation time and increased initial susceptibility, leading to a decrease in SAR. Interestingly, Dennis et al [2015] demonstrated that intracore magnetic interactions have an AMF amplitude-dependent effect on SAR. While more work is needed to fully elucidate the exact cause of SAR reduction in our present system, it appears that these clustered SPIOs provide no clear benefit over singly-dispersed cores for hyperthermia applications.

IV. CONCLUSION

In this work, we demonstrated a new method for producing self-assembled SPIO clusters in a simple coating reaction. This technique uses commercially available and FDA-approved DSPE-PEG, which provides an advantage over in-house synthesized block copolymers used by other groups. The decrease in SAR upon clustering observed here helps support the hypothesis that interactions between iron oxide cores limit the efficacy of hyperthermia treatments, which can be a factor following nanoparticle uptake into cells. Further, we found that this technique provides a means for producing efficient MRI contrast agents, as the R_2 value for the largest cluster formed from 15 nm SPIOs is among the highest ever reported. However, additional work is needed to characterize the *in vivo* stability and biodistribution of these clustered SPIOs before their full potential as MRI contrast agents can be realized.

ACKNOWLEDGMENT

The authors would like to thank Sheng Tong for providing the 15 nm SPIO cores. Magnetization measurements were conducted at the Advanced Materials Research Institute, University of New Orleans. This work was supported by the National Institutes of Health as a Program of Excellence in Nanotechnology Award (HHSN268201000043C to GB). TAM is supported by a National Science Foundation Graduate Research Fellowship (Grant No. DGE-1148903).

REFERENCES

Amsatd E, Gillich T, Bilecka I, Textor M, Reimhult E (2009). Ultrastable iron oxide nanoparticle colloidal suspensions using dispersants with catechol-derived anchor groups. Nano Letters, vol. 9, pp. 4042–4048. DOI: 10.1021/nl902212q [PubMed: 19835370]

Andreu I, Natividad E, Solozabal L, Roubeau O (2015). Same magnetic nanoparticles, different heating behavior: influence of the arrangement and dispersive media. J. Mag. Mag. Mat, vol. 380, pp. 341–346. DOI: 10.1016/j.jmmm.2014.10.114

Balasubramaniam S, et al. (2014). Toward design of magnetic nanoparticle clusters stabilized by biocompatible diblock polymers for T2-weighted MRI contrast. Langmuir, vol. 30, pp. 1580–1587. DOI: 10.1021/la403591z [PubMed: 24479874]

Berret JF, et al. (2006). Controlled clustering of superparamagnetic nanoparticles using block copolymers: design of new contrast agents for magnetic resonance imaging. J. Am. Chem. Soc, vol. 128, pp. 1755–1761. DOI: 10.1021/ja0562999 [PubMed: 16448152]

Branquinho LC et al. (2013). Effect of magnetic dipolar interactions on nanoparticle heating efficiency: implications for cancer hyperthermia. Sci. Rep, vol. 3, num. 2887. DOI: 10.1038/srep02887 [PubMed: 24096272]

Dennis CL, et al. (2015). Internal magnetic structure of nanoparticles dominates time dependent relaxation process in a magnetic field. Adv. Func. Mat, vol. 25, pp.4300–4311. DOI: 10.1002/adfm.201500405

Etheridge J, et al. (2014) Accounting for biological aggregation in heating and imaging of magnetic nanoparticles. Technology, vol. 2, pp. 214–228. DOI: 10.1142/S2339547814500198 [PubMed: 25379513]

Gonzalez-Weimuller M, Zeisberger M, Krishnan K (2009). Size-dependent heating rates of iron oxide nanoparticles for magnetic fluid hyperthermia. J. Mag. & Mag. Mat, vol. 321, pp. 1947–1950. DOI:10.1016/j.jmmm.2008.12.017

Gupta AK, Gupta M (2005). Synthesis and surface engineering of iron oxide nanoparticles for biomedical applications. Biomaterials, vol. 26, pp 3995–4021. DOI: 10.1016/j.biomaterials.2004.10.012 [PubMed: 15626447]

Haase C, Nowak U (2012). Role of dipole-dipole interactions for hyperthermia heating of magnetic nanoparticle ensembles. Phys. Rev. B, vol. 85, pp. 045435-1-5. DOI: 10.1103/PhysRevB.85.045435

Hugounenq P et al. (2012). Iron oxide monocrystalline nanoflowers for highly efficient magnetic hyperthermia. J. Phys. Chem C, vol. 116, pp. 15702–15712. DOI: 10.1021/jp3025478

Jun YW, et al. (2005). Nanoscale size effect of magnetic nanocrystals and their utilization for cancer diagnosis via magnetic resonance imaging. J. Am. Chem. Soc, vol. 127, pp. 5732–5733. DOI: 10.1021/ja0422155 [PubMed: 15839639]

Laurent S, Dutz S, Hafeli UO, Mahmoudi M (2011). Magnetic fluid hyperthermia: focus on superparamagnetic iron oxide nanoparticles. Adv. Coll. Int. Sci vol. 166, pp. 8–23. DOI: 10.1016/j.cis.2011.04.003

Lee N et al. (2012). Water-dispersible ferrimagnetic iron oxide nanocubes with extremely high r_2 relaxivity for highly sensitive in vivo MRI of tumors. Nano Lett., vol. 12, pp. 3127–3131. DOI: 10.1021/n13010308 [PubMed: 22575047]

Lee N, Yoo D, Ling D, Cho MY, Hyeon T, Cheon J (2015). Iron oxide based nanoparticles for multi-modal imaging and magnetoresponsive therapy. Chem. Rev. Article ASAP DOI: 10.1021/acs.chemrev.5b00112

Matsumoto Y, Jasanoff A (2008). T_2 relaxation induced by clusters of superparamagnetic nanoparticles: Monte Carlo simulations. Mag. Res. Im, vol. 26, pp. 994–998. DOI: 10.1016/j.mri.2008.01.039

Meteria ME, et al. (2014). Mesoscale assemblies of iron oxide nanocubes as heat mediators and image contrast agents. Langmuir, vol. 31, pp. 808–816. DOI: 10.1021/la503930s

Poselt E, et al. (2012). Relaxivity optimization of a PEGylated iron-oxide-based negative magnetic contrast agent For T2-weighted spin echo imaging. ACS Nano, vol. 6, pp. 1619–1624. DOI: 10.1021/nn204591r [PubMed: 22276942]

Sadat ME, et al. (2014). Effect of spatial confinement on magnetic hyperthermia via dipolar interactions in Fe_3O_4 nanoparticies for biomedical applications. Mat. Sci. Eng. C, vol. 42, pp. 52–63. DOI: 10.1016/j.msec.2014.04.064

Salas G et al. (2014). Modulation of magnetic heating via dipolar magnetic interactions in monodisperse and crystalline iron oxide nanoparticles. J. Phys. Chem. C vol. 118, pp. 19985–19994. DOI: 10.1021/jp5041234

Shtykova EV et al. (2007). Structure and properties of iron oxide nanoparticles encapsulated by phospholipids with poly(ethylene glycol) tails. J. Phys. Chem. C vol. 111, pp. 18078–18086. DOI: 10.1021/jp075235c

Stookey LL (1970). Ferrozine – a new spectrophotometric reagent for iron. Anal. Chem, vol. 42, pp. 779–781. DOI: 10.1021/ac60289a016

Sun S, et al. (2003). Monodisperse MFe_2O_4 (M = Fe, Co, Mn) nanoparticles. J. Am. Chem. Soc, vol. 126, pp. 273–279. DOI: 10.1021/ja0380852

Tong S, Hou S, Ren B, Zheng Z, Bao G (2011). Self-assembly of phospholipid-PEG coating on nanoparticles through dual solvent exchange. Nano Letters, vol. 11 pp, 3720–3726. DOI: 10.1021/nl201978c [PubMed: 21793503]

Urtizberea A, Natividad E, Arizaga A, Castro M, Mediano M (2010). Specific absorption rates and magnetic properties of ferrofluids with interaction effects at low concentrations. J. Phys. Chem. C, vol. 114, pp. 4916–4922. DOI: 10.1021/jp912076f

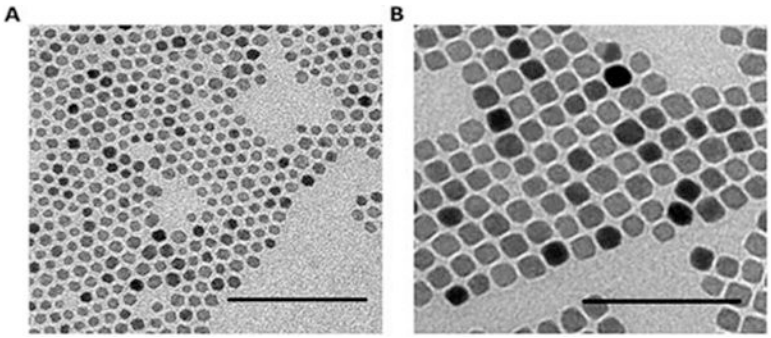

Fig. 1.
Representative TEM images of A) 8 nm and B) 15 nm iron oxide cores. Scale bar – 100 nm.

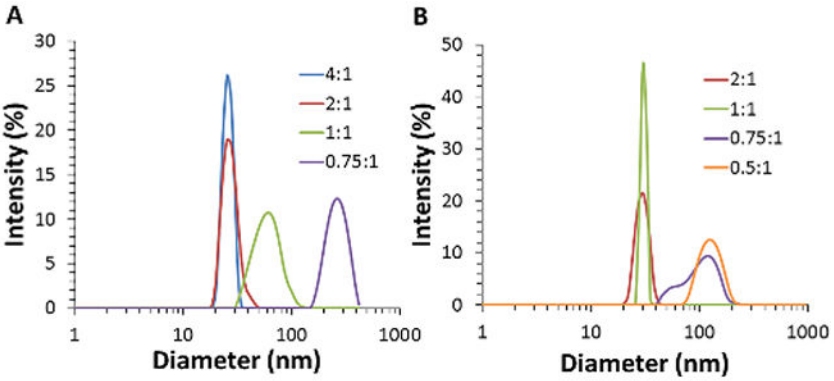

Fig. 2.

Size distributions from DLS of A) 8 nm and B) 15 nm SPIOs with different mass ratios of initial coating materials (DSPE-PEG:Fe).

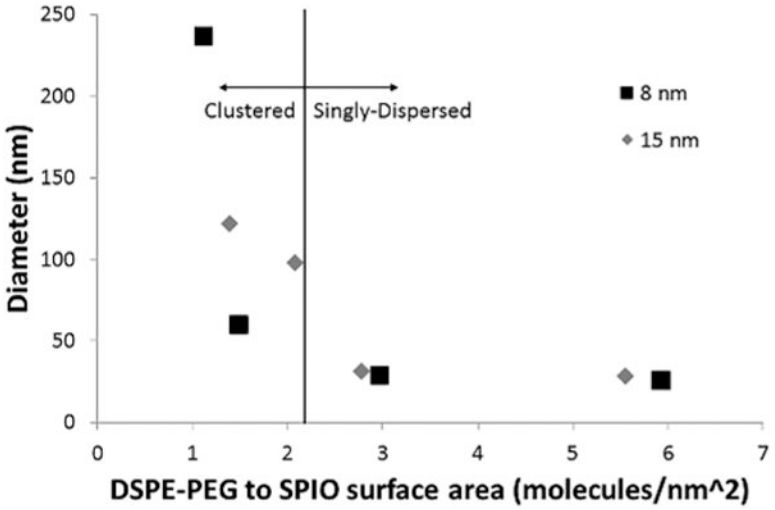

Fig. 3.

Average diameter as a function of the initial ratio of DSPE-PEG to core surface area for 8 nm and 15 nm iron oxide cores

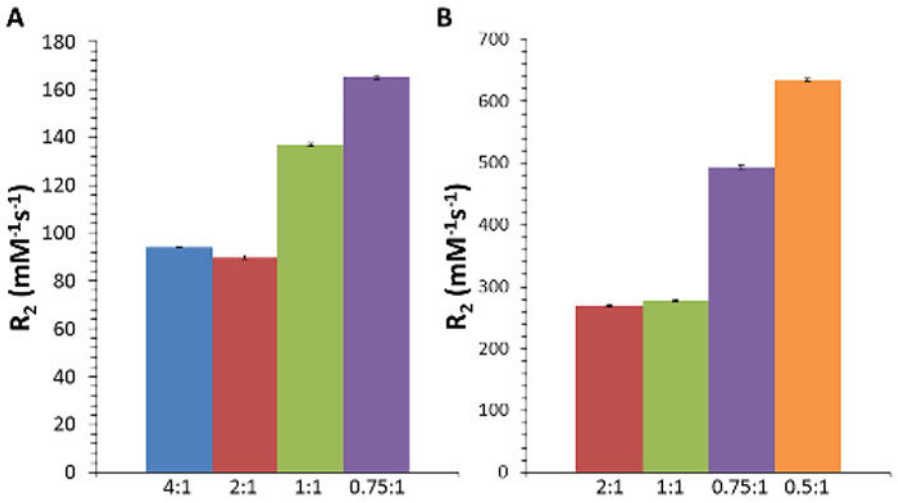

Fig. 4.

Calculated T2 relaxation rates for A) 8 nm and B) 15 nm SPIO cores coated with different DSPE-PEG:Fe ratios (mean ± s.d., n=3).

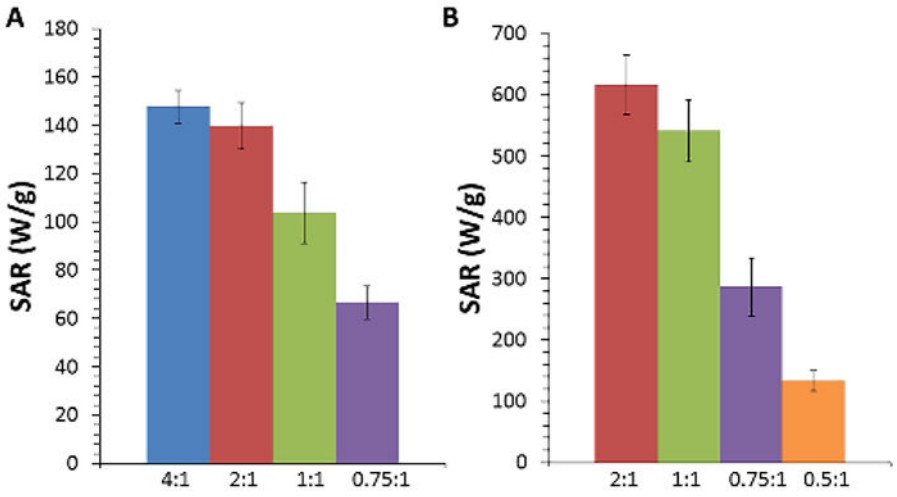

Fig. 5.

Calculated specific absorption rates for A) 8 nm and B) 15 nm iron oxide cores coated with different DSPE-PEG:Fe ratios exposed to an alternating magnetic field (23.77 kA/m, 355 kHz) (mean ± s.d., n=3).

Table 1

Average hydrodynamic diameters and percent polydispersity (%PD) of A) 8 nm and B) 15 nm iron oxide cores coated with different DSPE-PEG:Fe ratios (mean ± s.d., n=3)

A	Diameter (nm)	%PD		B	Diameter (nm)	%PD
4:1	25.8 ± .1	0.12		2:1	28.2 ± .2	0.07
2:1	28.9 ± .1	0.14		1:1	31.1 ± .1	0.11
1:1	60.4 ± .4	0.22		0.75:1	97.7 ± 1.1	0.18
0.75:1	237.1 ± 1.9	0.24		0.5:1	122.1 ± .9	0.18